Wisbey, D. S. et al. (2019) Dielectric loss of boron-based dielectrics on niobium resonators. Journal of Low Temperature Physics, 195(5-6), pp. 474-486.

There may be differences between this version and the published version. You are advised to consult the publisher's version if you wish to cite from it.

http://eprints.gla.ac.uk/187357/

Deposited on: 28 May 2019

Enlighten – Research publications by members of the University of Glasgow
http://eprints.gla.ac.uk

Noname manuscript No.
(will be inserted by the editor)

Dielectric Loss of Boron-Based Dielectrics on Niobium Resonators

David S. Wisbey · Michael R. Vissers · Jiansong Gao · Jeff S Kline · Martin O. Sandberg · Martin P. Weides · M. M. Paquette · S. Karki · Jacob Brewster · Dheyaa Alameri · Irma Kuljanishvili · Anthony N. Caruso · Dave P. Pappas

Received: date / Accepted: date

Abstract Advanced solid state quantum bits (qubits) are likely to require a variety of dielectrics for wiring crossovers, substrates, and Josephson junctions. Microwave superconducting resonators are an excellent tool for measuring the internal dielectric loss of materials. We report the dielectric loss of boron-based dielectric films using a microwave coplanar waveguide (CPW) resonator with heterostructure geometry. Power-dependent internal quality factors of magnetron-sputtered boron carbide (B_4C) and boron nitride (BN) were measured and are compared to silicon oxide (SiO_2), a common material used in wiring crossovers. The internal dielectric loss due to two-level systems for B_4C and BN is less than silicon dioxide (SiO_2), which demonstrates the existence of low loss sputtered materials. We also found that niobium (Nb) CPW resonators suffer a decrease in internal quality factor after deposition of B_4C at temperatures above 150°C. This result is consistent with the idea that the oxidation of the surface of the superconducting metal can contribute to loss in a device.

Keywords Superconducting resonator · low temperature loss · two-level systems · boron nitride · boron carbide

This work was funded by the U.S. government, Office of the Director of National Intelligence (ODNI), Intelligence Advanced Research Projects Activity (IARPA), and the NIST Quantum-based Sensors and Measurements Initiative. All statements of fact, opinion, or conclusions contained herein are those of the authors and should not be construed as representing the official views or policies of ODNI or IARPA. UMKC acknowledges financial support from the Defense Threat Reduction Agency under grant no. HDTRA1-10-1-0092.

D. Wisbey, J. Brewster, D. Alameri, I. Kuljanishvili
Saint Louis University, Department of Physics, St. Louis Missouri, USA
Tel.: 314-882-4312 Fax: 314-977-8384
E-mail: david.wisbey@slu.edu ORCID ID: https://orcid.org/0000-0001-6376-6052

M. Vissers, J. Gao, J. Kline, D. P. Pappas
National Institute of Standards and Technology, Boulder Colorado, USA

M. Sandberg
IBM, Armonk, New York, NY, USA

M. Weides
School of Engineering, University of Glasgow, Glasgow G12 8QQ, UK

M. Paquette, S. Karki, A. N. Caruso
University of Missouri-Kansas City, Department of Physics and Astronomy, Kansas City Missouri, USA

1 Introduction

Evaluating the loss in dielectric materials at very low temperatures is important for the continued advance of superconducting circuits used in quantum information processing (QIP). Currently, materials used in solid state heterostructure devices are a limiting factor, preventing the realization of a scalable quantum computer. Microwave resonators are an excellent tool for studying the various properties, most importantly the loss, of materials to be used for fabricating qubits. This is because they are both an intrinsic component and a good test bed for loss measurements [1].

The dielectric loss of boron carbide (B_4C) and boron nitride (BN) was measured using microwave resonators. Boron nitride and boron carbide are some of the hardest materials in the world after diamond and cubic BC_2N [2]. This hardness is associated with a high electron bond strength, a lower amount of unpaired electrons, a strong tendency for covalent bond formation, and a lack of dangling bonds. Dangling bonds at the surfaces

of metal electrodes and dielectric interfaces have been associated with decoherence and increased *1/f* noise in superconducting microwave devices [3,4]. Boron nitride is a particularly interesting material because it has tunable properties such as band gap, stoichiometry, and bond strength [5].

Microwave loss in a dielectric is referred to as $\delta_i = 1/Q_i$ where Q_i is the internal quality factor. The internal quality factor is defined as the energy stored in the resonator divided by energy lost to internal sources of the device. Internal sources of loss can include a variety of things; however, at low temperatures and low microwave power, it is often dominated by two-level systems [6]. A previously established standard for testing and quantifying the microwave loss of new materials in circuits for quantum information processing (QIP)[7–10] was used.

This paper shows that B_4C and BN have a lower dielectric loss than SiO_2 grown with electron cyclotron resonance (ECR). Wiring crossovers made of SiO_2 were commonly used previously. While the measured loss is larger than that obtained for the lowest loss deposited dielectric a-Si:H [7], boron-based dielectric can be sputter-deposited at room temperature, which is advantageous. The material a-Si:H usually requires growth at an elevated temperature of around 250°C [11]. Dielectrics that require heating the sample can cause adverse effects, e.g., hydrogen or silicon may get incorporated into the superconductor or the crystal structure of the underlying layers may change. We also show that heating a niobium resonator causes the quality factor of the resonator to drop and the resonance frequency to change.

2 Experimental

2.1 Microwave Measurement Setup

An adiabatic demagnetization refrigerator (ADR) was used to conduct the low temperature measurements. The system had a base temperature of less than 80 mK [12], as measured using a RuO_2 sensor attached to the sample holder. The experimental setup used to make RF measurements is shown in Fig. 1. Measurements consisted of transmission S_{21} using a 1 GHz - 20 GHz vector network analyzer (VNA). The input microwave signal was attenuated by 70 dB before reaching the device. The various attenuators are shown at the different temperature stages in Fig 1. The signal passed through four DC blocks, two at the 500 mK stage and two at the 50 mK stage. The transmitted signal from the sample was sent to the 500 mK stage where it passed through a bias tee, to cool the center conductor of the coaxial cable, and a directional circulator, and then to a high

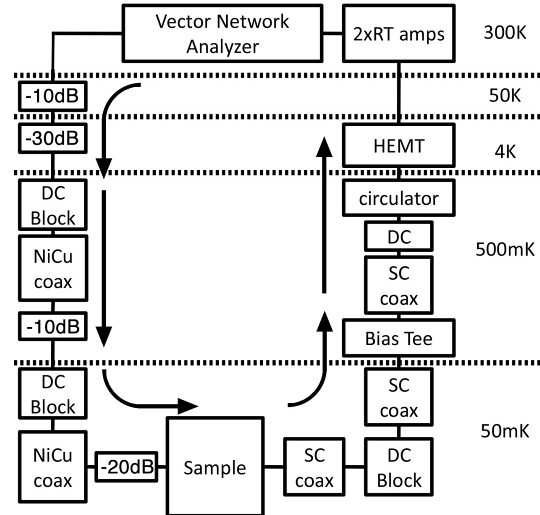

Fig. 1 Schematic of the microwave measurement setup. The arrows indicate the direction of the microwave signal flow. The sample was at 80 mK while the bias T and directional circulator were at the 500 mK stage during measurement. There were four DC blocks, two at the 50 mK stage, and two at the 500 mK stage. The HEMT amplifier was at 4K. The attenuators were distributed over the various temperature stages as shown, with two amplifiers at room temperature.

electron mobility transistor (HEMT) amplifier at the 4 K stage. The HEMT amplifier gave about 40 dB amplification over the bandwidth used.

Another 30 dB amplification was achieved with external room temperature amplifiers. Because the quarter wave CPW resonators are coupled to a continuous CPW feedline, we measure a dip in the transmitted power at the resonance frequency of each resonator. This paper follows a well demonstrated technique [6–10,12] to measure the loss tangent of dielectric materials. Coplanar waveguides are advantageous for materials studies because they are well understood, straightforward to analyze, and the loss, $1/Q_i$, is additive, and thus easy to separate into different components [7,15]. Measurements of the TLS loss were determined using both the power and temperature dependence of resonance [16].

2.2 Fabrication and Resonator Design

The low temperature dielectric loss of our samples was measured using quarter wave coplanar waveguide (CPW) resonators. The SiO_x and B_4C data were measured using a CPW resonator composed of 200 nm of niobium (Nb) on a sapphire substrate. Devices with BN were measured with a 200 nm Nb resonator on an intrinsic Si(100) wafer. Sapphire was chosen for the B_4C devices so that the dielectric could be deposited at high temperature without affecting the substrate. This allowed B_4C

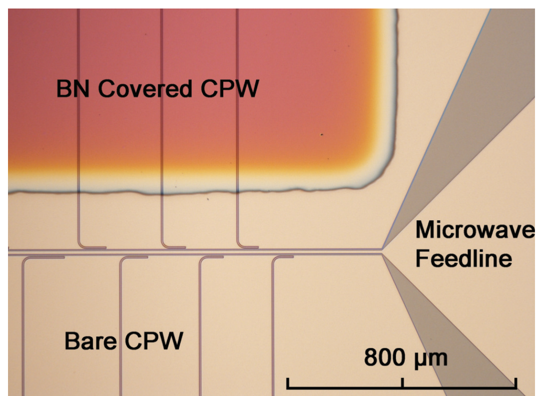

Fig. 2 Frequency multiplexed niobium quarter wave coplanar waveguide (CPW) resonators covered with 300 nm of deposited BN.

samples grown at high and low temperatures to be compared. The niobium CPW resonators were capacitively coupled to a continuous CPW feedline for transmission measurements. They were etched using SF_6 at low RF power [12]. The samples were grown on 76 mm (3") wafers of either c-plane sapphire or intrinsic Si(100) with a resistivity of 17 kΩ-cm. The sapphire substrates were annealed in a tube furnace for 20 h at 1100°C in an oxygen atmosphere *in situ* to prepare the surface. After annealing the substrates, the surface is much smoother and more crystalline, as described previously [13]. For the Si substrates, prior to deposition, the native oxide was removed using HF as described previously [12]. A 200 nm thick Nb film was then grown in a UHV chamber at room temperature. No RF plasma clean was used prior to deposition of the Nb. To maximize the effect of the two-level systems (TLSs) in the dielectric material [8] and avoid trapped magnetic flux in the CPW line [8,14], we chose a center line width of 3μm and a gap width of 2 μm, as described previously [6,8,12].

Fourteen resonators were frequency multiplexed with seven on each half of a die separated by the microwave feedline. Resonators were divided in two halves on a die in order to distinguish between covered and uncovered devices. Figure 2 (a) shows the CPW resonators on either side of the microwave feedline. As shown in Fig. 2 (a), the coupling capacitors had no deposited materials. This sample has 300 nm of BN covering all the resonators above the feedline.

The microwave resonators had a resonance frequency in the range of 4.5 GHz to 9.0 GHz. The CPW resonators were designed in pairs so that the resonance frequencies of the pair were separated by 50 MHz. Each pair was separated from the other pairs of CPWs by at least 500 MHz. This was done so that individual resonators could be easily distinguished. The CPW resonators had a coupling quality factor Q_c of 175,000 to 500,000. In this study, a careful measurement of the kinetic inductance was not made. This lead to higher uncertainty in the calculations of the effective dielectric constant and the filling factors. For the resonators with BN and SiO_2 deposited on the surface, the shift in resonance frequency from the theoretical value for an uncovered resonator was less than 2%, meaning they had a small kinetic inductance fraction.

For the samples with B_4C deposited, we found that the measured resonance frequency deviated from the theoretical value for an uncovered resonator by almost 10%. With a high kinetic inductance, the effective dielectric constant reported has a high uncertainty. Depositing dielectric material on the resonators increased the effective dielectric constant, which shifted the resonance frequency lower, typically by a few hundred megahertz. For example, one resonator covered by 250 nm of B_4C had a resonance frequency (f_r) of 5.23 GHz, whereas a bare Nb resonator had a designed resonance frequency of f_r=5.65GHz.

2.3 Dielectric Deposition

Two different thicknesses of dielectric films for the SiO_x and the BN sample were used in this study, as listed in Table 1. For the B_4C sample, only one thickness was used, 250 nm, due to difficulties growing thicker films. The BN target had a purity of 99.99%. The BN film was grown with argon (Ar) and nitrogen (N) gas flowing into the chamber during sputter with a rate of 15 sccm for N and Ar at a pressure of 0.4 Pa. The sample was at room temperature. Both thin films of B_4C and BN were grown onto the niobium coplanar waveguides described previously in this paper.

The thin film of SiO_2 was grown using a commercially available electron cyclotron resonance (ECR) machine at low power. A shadow mask was machined out of molybdenum (Mo) that enclosed the sample with an opening cut in it so that B_4C, BN, and SiO_2 would cover half the resonators (see Fig. 2). Wire-bond pads, the microwave feedline, and half the resonators on the other side of the die were completely covered to ensure material was only deposited where intended. The opening in the shadow mask was 350 μm away from the transmission line. The uncovered resonators were used as control devices. This is useful for monitoring the dielectric constant of the substrate and material properties of the superconducting metal. The dielectric loss of each device was measured for covered and uncovered devices. Prior to deposition, bare Nb devices had a low power low temperature loss of approximately 8×10^{-6}. This ensured the resonators were not destroyed during processing and that measurements were consistent.

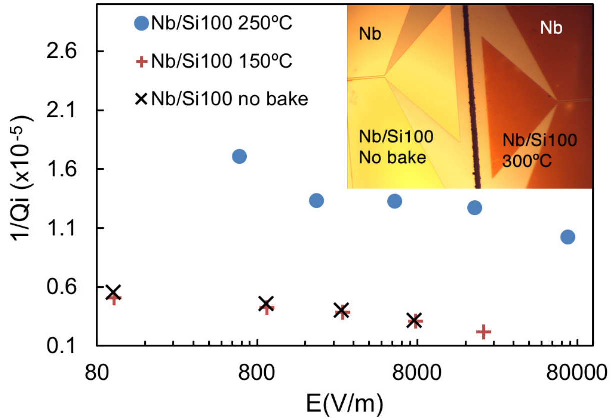

Fig. 3 Inverse of the internal quality factor for niobium resonators with no deposited material heated in a low oxygen environment. The inset shows two bare Nb resonators on intrinsic Si(100). The left resonator in the inset had no annealing, while the right resonator was annealed at 300°C.

The internal dielectric loss of the deposited material on resonators could then be obtained.

Thin films of B_4C, 250 nm in thickness, were deposited by magnetron sputtering from a hot pressed B_4C target with argon process gas at substrate temperatures of 20°C and 350°C. The 102 mm target was manufactured with an epoxy bonded copper backing plate. During deposition, the target power was kept to 50 W and ramped at 1 W/min to prevent cracking, yielding a deposition rate of 0.9 Å/min. X-ray photoemission demonstrated argon and oxygen incorporation at less than 5% of the $B_{3.9}C$ stoichiometry for both samples.

We found Nb resonators with B_4C deposited at 350 °C had a quality factor that was to low too be measured. One possible reason for the decrease in quality factor could be oxidation of the Nb in the resonator. Previous studies showed that the surface of Nb 3d RF cavities begins to oxidize above 100°C and decreases the performance [20–23]. We also found that as Nb resonators were heated in a chemical vapor deposition (CVD) system there was an increase in the dielectric loss as shown in Fig. 3. Prior to heating, the CVD chamber was pumped for 20 minutes using a mechanical roughing pump, then the CVD chamber was purged for 10 minutes with Ar gas (600 sccm) while being pumped. The CVD was then brought to the various temperatures within 20 minutes and kept at those temperatures for an additional 30 minutes.

During heating, the CVD was evacuated using a mechanical roughing pump. For the samples heated at room temperature and at 150 °C, there was no change in the dielectric loss of the device as shown in Fig. 3. For samples heated to 250°C, the dielectric loss increases to over 10^{-5} as shown in Fig. 3. The inset of Fig. 3 also shows a distinct change in the color of the Nb for a resonator annealed at 300°C. The pristine resonator on the left in the inset had a distinctly golden silver hue, while the resonator that was annealed at 300°C on the right had a dark reddish brown hue. What this shows is that when Nb microwave resonators are heated above 150°C, there is a change in the Nb and an increase in internal loss. Most likely, this is due to oxidation of the Nb, as reported previously [20–24]. Careful measurement of the critical temperature (T_c) of the devices shown in Fig. 3 were not made. However the changes in the T_c of Nb after heating were previously reported [24]. Prior to deposition of amorphous silicon (a-Si) using PECVD when Nb was heated to 250°C, they measured a decrease in T_c. This can be attributed to the fact that oxygen and hydrogen migrate from the surface to the bulk of the Nb and cause an expansion of the crystal lattice. The findings in this paper compliment the earlier work [24] and show that not only does heating Nb cause a structural change in Nb and a decrease in the T_c, but it also leads to an increase in internal loss of the device.

For bare Nb resonators heated to 250°C, there was a shift in the resonance frequency by about 2 GHz. Whereas, the sample heated to 150° had only a slight shift to a lower resonance frequency of less than 100 MHz. Since the device geometry hasn't changed, either the dielectric material under the metal changed or the metal itself changed.

3 Power Dependence of Loss

Fig. 4 shows the loss tangent of two different samples of B_4C (250 nm) and a bare Nb resonator. The data points for the two samples are shown as circles and squares. The power fit of the data is shown as a dashed lined using Eq. 2. We find that δ_i for the uncovered Nb resonator was 8.2 $\times 10^{-6}$. This shows that the dielectric films were effectively masked. Also, Auger electron spectroscopy (AES) showed no evidence of the deposited dielectric on the covered side of the wafer. However, there was a change in resonance frequency with a corresponding change in the effective dielectric constant as calculated with Eq. 3. Deviations in the dielectric constant can be used as an indicator of issues with the device as a whole.

The intrinsic loss due to two level systems, δ^0_{tls}, was measured using the internal loss vs. the power. In order to find δ^0_{tls}, the internal quality factor, Q_i, must first

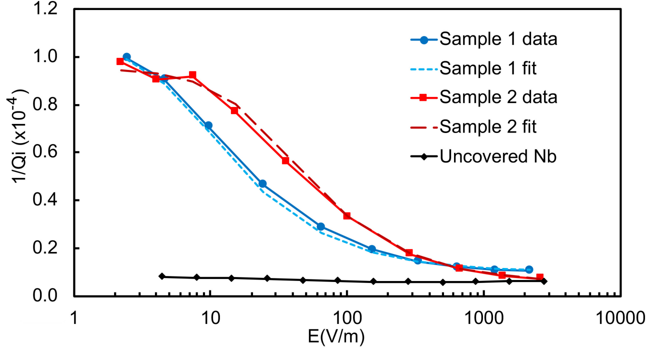

Fig. 4 Internal loss of two resonators with deposited B_4C and one bare Nb resonator on sapphire. Sample 1 and 2 both had B_4C grown at room temperature. The loss tangents for both samples with deposited B_4C appear to converge to the same value for low power. Uncovered Nb on sapphire is shown in black for comparison.

Table 1 Comparison of internal loss at low power and temperature using $F\delta^0_{\text{TLS}}$ using Eq. 4 and Eq. 2. The first column is the deposited material, the second is the thickness of the deposited material on Nb, δ_i is the measured internal loss, ε_{dep} is the dielectric constant of the deposited material, F is the filling factor, and $F\delta^0_{\text{TLS}}$ temp is the intrinsic loss due to TLSs times the filling factor taken from the temperature dependent data. The column $F\delta^0_{\text{TLS}}$ power was taken from a power fit of the data. Parentheses indicate the uncertainty in the last digit.

Material	thickness(nm)	$\delta_i(\times 10^{-4})$	ε_{dep}	F	$F\delta^0_{\text{TLS}}$ temp $(\times 10^{-4})$
B_4C/Nb	250(10)	1.0	4(2)	0.04(2)	1.50(4)
BN/Nb	170(5)	0.23	3.2(5)	0.019(4)	0.35(5)
BN/Nb	300(5)	0.516	3.5(3)	0.034(4)	0.57(1)
SiO_2/Nb	450(5)	1.73	3.5(9)	0.05(2)	2.02(1)
SiO_2/Nb	900(5)	2.20	3.4(9)	0.08(2)	4.00(1)

be found. For a resonator, Q_i, can be found by solving the equation

$$\frac{1}{Q_m} = \frac{1}{Q_c} + \frac{1}{Q_i}. \tag{1}$$

where Q_m is the measured quality factor and Q_c is the coupling quality factor. Both Q_m and Q_c were extracted from the measured transmission S_{21} data using the circle fit method [6,12,17]. A microwave electromagnetic simulator was also used to calculate Q_c [6] based on the method of Ben Mazin [25]. The measured values of Q_c obtained from the circle fit method were lower than the designed values by up to 33%. This discrepancy is well known and could be due to the proximity to other resonators or other factors introduced during fabrication [25].

Internal loss, $1/Q_i$, as a function of electric field strength is shown in Fig. 4. Eq. 1 is used to separate the internal quality factor from the measured quality factor. Internal loss $\delta_i = 1/Q_i$ is composed of two terms, $\delta_i = \delta^0_{tls} + \delta_0$, where δ^0_{tls} is the power dependent loss due to two-level systems, and δ_0 is the background loss, which is power independent [18]. The internal loss is fit in Fig. 4 using the equation

$$\frac{1}{Q_i} = \frac{F\delta^0_{tls} tanh(\frac{\hbar\omega}{2k_BT})}{\sqrt{1 + (\frac{E}{E_c})^\beta}} + \delta_0 \tag{2}$$

where F is the filling factor of the dielectric in the CPW gap, $\hbar$ is Planck's constant, k_B is Boltzman's constant, E is the power in the resonator, and E_c is a fitting paramterter associated with the critical power above which the TLSs are "saturated" [16]. Figure 4 shows that there is good agreement between measured internal quality factor data, circles and squares, and the fitting function Eq. 1, dashed lines. We found that the two samples of B_4C had different values of E_c using Eq. 1: 7 for sample 1 and 25 for sample 2 shown in Fig.4. This difference in value could be due to variations in the deposition of B_4C. Variation in sample fabrication is unfortunately a much bigger issue that plagues many devices in quantum information. To realize a quantum computer, reproducibility among devices will be a key in large scale arrays of qubits. The filling factor was calculated by taking the capacitance in the region with the deposited dielectric material, divided by the total capacitance of the device. The results for this method of fitting for all materials in this study are listed in Table 1. Capacitance for each region (the substrate, sputter deposited material and vacuum) were calculated according to the references [7,19]. When calculating the capacitance of a device, it is necessary to know the effective dielectric constant, ε_{eff}. We found ε_{eff} using the equation

$$\varepsilon_{eff} = \frac{c}{4l}\frac{1}{f_r} \tag{3}$$

where c is the speed of light, l is the physical length of the resonator, and f_r is the resonance frequency of the CPW. The length of the resonators l was known from the design of the CPW. The dielectric constant of the material, ε_r, was determined using ε_{eff} and conformal mapping described by Simmons [19].

The intrinsic dielectric loss tangent δ^0_{tls}, the dashed lines shown in Fig. 4, can be extracted from Eq. (2) by fitting the data for $1/Q_i$ according to the references [1,16,18]. The value of the exponent $\beta = 1.6$, was the best value for fitting the data in agreement with the literature [1,18].

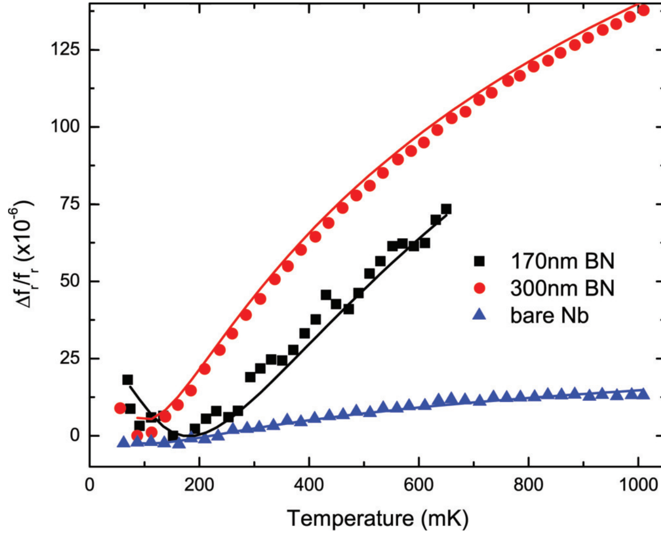

Fig. 5 The relative resonance frequency vs temperature shift for BN is shown. Dielectric loss was measured for the deposited BN as described in the experimental setup and shown in the figure. Shapes represent the actual data points while the solid lines are fits of the data using Eq. 4.

4 Temperature Dependence of Loss

The zero-temperature loss due to two-level systems, δ^0_{tls} can be measured at a fixed high power, typically -70 dBm or an electric field strength of E $\approx$ 8000 V/m, using the temperature dependence of the resonance frequency,

$$\frac{\Delta f_r(T)}{f_r} = F\delta^0_{tls}[\Re\Psi(\frac{1}{2} - \frac{\hbar\omega}{2ik_BT}) - \log(\frac{\hbar\omega}{2\pi k_BT})] \quad (4)$$

where Δf_r is the frequency shift, f_r is the resonance frequency at low temperature, ω is the angular frequency $2\pi f$, T is the temperature, and $\Re\Psi$ is the real part of the digamma function. Fitting using equation 4 was taken from ref. [6]. For consistency, δ^0_{tls} from the temperature dependent data was checked and found to be consistent with that found from the power dependent data as shown in Table 1. In Fig. 5 the measured relative resonance frequency as a function of temperature is fit using Eq. 4 for samples covered with BN.

Extracting the internal dielectric loss, δ^0_{tls}, using Eq. 4 is much easier than using the power fit method since low power scans are not required, as discussed in the literature [6].

5 Results and Discussion

Using Eq. 4 to fit the frequency versus temperature data, values for $F\delta^0_{tls}$ are given in Table 1. We found that B_4C has a zero-temperature TLS loss of $F\delta^0_{tls}$ of between 1×10^{-4} and 1.5×10^{-4}, and BN has a zero-temperature TLS loss of $F\delta^0_{tls} = 0.60 \times 10^{-4}$ as shown in Table 1. Both of these two materials had a lower zero-temperature TLS loss than that of SiO_2 by roughly a factor of 2 to 3. We also found that as the thickness of the BN and SiO_x increased, $F\delta^0_{tls}$ increased as well. For BN and SiO_x, if $F\delta^0_{tls}$ is divided by F, then one finds a constant value of δ^0_{tls}=1.7(1)x10^{-3} and δ^0_{tls}=4.3(2)x10^{-3} respectively (the parentheses indicate the uncertainty in the last digit), implying that TLSs are distributed throughout the amorphous dielectric layer as listed in Table 1.

The main mechanism known that causes dielectric loss at low temperature and low power is two-levels systems [29–31]. Two-level systems (TLSs) have an electric dipole and are associated with dangling bonds. For example, in SiO_2 and SiN_x, the loss is attributed to the strong polar microwave absorption from molecules such as OH^- or other impurities with an electric dipole moment such as F^- and Cl^- atoms. Paik *et al.* [10] observed a correlation between the number of NH_2 molecules and the dielectric loss in their SiN_x films. These impurities act like two-level systems that become unsaturated at low temperature and power and thus begin absorbing power. Polar molecules like NH_2 that are present in SiN due to the growth process, provide a clear physical example of how a two-level system could absorb power from a microwave circuit. As the electric field of the microwave acts on the dipole moment of these molecules, it can absorb the microwave photon and be excited into a rotational or vibrational state. The molecule has a certain lifetime in the excited state and then will decay via microwave photons or phonons.

For B_4C and BN, a considerable numbers of defects are known to be distributed throughout magnetron sputtered films depending on the growth conditions. Werheit *et al.* [32,33] point out that B_4C contains a high level of substitutional disorder, thereby creating electronic defects in the material. These defects act as dopants, i.e. electric dipoles, as reported by Schmechel *et al.* [34]. Due to the amorphous nature of the magnetron sputtered BN and B_4C, there is a broad spectrum of energy activation of these defects; thus, these defects can act as the two level systems that can absorb energy at low power and low temperature in the RF regime. With respect to the materials presented in this study, it means that if defects could be removed from B_4C and BN, the loss in these dielectric materials could be removed.

This work also speaks to a bigger challenge in device fabrication [26]. Growing crystalline Josephson junctions in a qubit has been a goal of many research groups over the years. This was successful to a certain extent [27], but did not completely solve the problem of TLSs in barriers. What this work shows is that the fabrication process in producing crystalline materials could be

causing other issues in the devices. Most likely, producing the crystalline element of a device, such as a Josephson junction in a qubit, will require annealing the entire device. Since annealing a device increases the likelihood of oxidation of metallic layers, this could be problematic for incorporating crystalline materials in devices for quantum computing. Recently, Kumar *et al.* [28] found strong evidence that molecular oxygen at the superconducting metal surface can play a large role in unwanted noise in superconducting devices. One important question then is whether or not molecular oxygen incorporated into a material, such as sputter-deposited B_4C, could also lead to increased internal loss.

This research shows further studies on B_4C and BN are warranted since these materials have variable mechanical and electronic properties that depend on their growth conditions [5, 35]. As with SiO_2 and SiN_x, it may be possible to improve the loss for B_4C and BN dielectrics by altering the sputter deposition recipe. Neither of these materials have had extensive studies done on the dielectric loss in the context of devices for quantum computing. One possibility would be to vary the sputter deposition conditions with which B_4C and BN are grown. Alternatively, using a different superconducting material such as aluminum, and annealing the devices during or after deposition could remove impurities and increase order in the deposited materials. However, in the case of BN, if the substrate is heated, it is known that BN will not stick to the surface. The datasets generated during and/or analyzed during the current study are available from the corresponding author on reasonable request.

6 Conclusion

In conclusion, we have shown B_4C has a zero-temperature TLS loss of $F\delta^0_{tls}$ of between 1×10^{-4} and 1.5×10^{-4}, while boron nitride has a zero-temperature TLS loss of $F\delta^0_{tls} = 0.60 \times 10^{-4}$ which are both lower than that of SiO_2 by roughly a factor of 2 to 3. Boron nitride (BN) and boron carbide (B_4C) are straightforward to grow using sputter deposition which makes them very attractive for a wiring crossover. We also found that deposition of dielectric materials at elevated temperatures, above 150°C, can have unwanted effects on the circuit as a whole such as oxidation of the superconducting metal, a decrease in quality factor, and a change in resonance frequency of the devices.

References

1. J. M. Sage, V. Bolkhovsky, W. D. Oliver, B. Turek, P. B. Welander, J. Appl. Phys. **109**,063915 (2011)
2. V. L. Solozhenko, N. A. Dubrovinskaia, L. S. Dubrovinsky, Appl. Phys. Lett. **85**, 1508, (2004)
3. R. Sousa, Phys. Rev. B **76**, 245306 (2007)
4. F. Yoshihara, Y. Nakamura, J. S. Tsai, Phys. Rev. B **81**, 132502 (2010)
5. M. D. Wiggins, C. R. Aita, J. Vac. Sci. Tech. **2**, 322 (1984)
6. J. Gao, Caltech Ph.D. thesis (2008)
7. A. D. O'Connell, M. Ansmann, R. C. Bialczak, M. Hofheinz, N. Katz, E. Lucero, C. McKenney, M. Neeley, H. Wang, E. M. Weig, A. N. Cleland, and J. M. Martinis, Appl. Phys. Lett. **92**, 112903 (2008)
8. J. Gao, M. Daal, A. Vayonakis, S. Kumar, J. Zmuidzinas, B. Sadoulet, B. A. Mazin, P. K. Day, H. G. Leduc, Appl. Phys. Lett. **92**, 152505 (2008)
9. R. Barends. H. L. Hortensius, T. Zijlstra, J. J. A. Baselmans, S. J. C. Yates, J. R. Gao, T. M. Klapwijk, Appl. Phys. Lett. **92**, 223502 (2008)
10. H. Paik, K. D. Osborn, Appl. Phys. Lett. **96**, 072505 (2010)
11. A. Brunoa, S.T. Skacelc, Ch. Kaiserc, S. Wu?nschc, M. Siegelc, A.V. Ustinovd, M.P. Lisitskiya, Physics Procedia textbf36, 245 ? 249 (2012)
12. D. Wisbey, J. Gao, M. Vissers, Fabio C. S. da Silva, J. S. Kline, L. Vale, D. Pappas, J. Appl. Phys. **108**, 093918 (2010)
13. A. Megrant, C. Neill, R. Barends, B. Chiaro, Y. Chen, L. Feigl, J. Kelly, E. Lucero, M. Mariantoni, P. O'Malley, D. Sank, A. Vainsencher, J. Wenner, T. White, Y. Yin, J. Zhao, C. Palmstrϕm, J. Martinis, A. Cleland, Appl. Phys. Lett. **100**, 113510 (2012)
14. C. Song, T. W. Heitmann, M. P. DeFeo, K. Yu, R. McDermott, M. Neeley, J. M. Martinis, B. L. T. Plourde, Phys. Rev. B **79**, 174512 (2009)
15. M. Göppl, A. Fragner, M. Baur, R. Bianchetti, S. Filipp, J. M. Fink, P. J. Leek, J. Appl. Phys. **104**, 113904 (2008)
16. D. P. Pappas, M. R. Vissers, D. S. Wisbey, J. S. Kline, J. Gao, IEEE Trans. Appl. Supercond. **21**, 871 (2011)
17. S. Probst, F. B. Song, P. A. Bushev, A. V. Ustinov, and M. Weides Rev. Sci. Instrum. 86, 024706 (2015)
18. H. Wang, M. Hofheinz, J. Wenner, M. Ansmann, R. Bialczak, M. Lenander, E. Lucero, M. Neeley, A. O'Connell, D. Sank, M. Weides, A. Cleland, and John Martinis, Appl. Phys. Lett. **95**, 233508 (2009)
19. R. N. Simons, "Coplanar Waveguide Circuits, Components, and Systems" Willey Series in Microwave and Optical Engineering, Kai Chang, Series Editor (2001) By John Wiley and Sons, ISBN 0-471-16121-7
20. O. Hellwig, H. Zabel, Physica B, **283**, 228 (2000)
21. O. Hellwig, H. W. Becker, H. Zabel, Phys. Rev. B, **64**, 233404 (2001)
22. T. Proslier, J. Zasadzinski, J. Moore, M. Pellin, J. Elam, L. Cooley, C. Antoine, J. Norem, K. E. Gray, Appl. Phys. Lett. **93**, 192504 (2008)
23. J. Halbritter, Appl. Phys. A **43**, 1-28 (1987)
24. A. Bruno, P. Mengucci, L. V. Mercaldo, M. P. Lisitskiy, Phys. Procedia **36**, 239-244, (2012)
25. B. Mazin, Caltech Ph.D. thesis (2008)
26. S. Oh, K. Cicak, J. S. Kline, M. A. Sillanp, K. D. Osborn, J. D. Whittaker, R. W. Simmonds, D. P. Pappas, Phys. Rev. B **74**, 100502(R) (2006)
27. M. Weides, J. S. Kline, M. Vissers, M. Sandberg, D. S. Wisbey, B. R. Johnson, T. Ohki, and D. P. Pappas, Appl. Phys. Lett. 99, 262502 (2011)
28. P. Kumar, S. Sendelbach, M. A. Beck, J. W. Freeland, Zhe Wang, H. Wang, C. C. Yu, R. Q. Wu, D. P. Pappas, R. McDermott, Phys. Rev. Appl. **6**, 041001 (2016)
29. W. A. Phillips, Rep. Prog. Phys. **50**, 1657 (1987)

30. M. Von Schickfus, S. Hunklinger, Phys. Lett. **64**, 144 (1977)
31. M. Von Schichfus, S. Hunklinger, J. Phys. C: Solid State Phys. **9**, L439 (1976)
32. H. Werheit, H. W. Rotter, F. D. Meyer, H. Hillebrecht, S. O. Shalamberdze, T. G. Abzianidze, G. G. Esadze, J. Solid State Chem. **177**, 569 (2004)
33. H. Werheit, T. Au, R. Schmechel, J. Solid State Chem. **154**, 79 (1999)
34. R. Schmechel, H. Werheit, J. Phys.: Condens. Matter **11**, 6803 (1999)
35. L. G. Jacobsohn, M. Nastasi, Surf. Coat. Technol. **200**, 1472 (2005)